Estuarine, Coastal and Shelf Science 90 (2010) 61–72

Contents lists available at ScienceDirect

Estuarine, Coastal and Shelf Science

journal homepage: www.elsevier.com/locate/ecss

How do uncertainties in hurricane model forecasts affect storm surge predictions in a semi-enclosed bay?

Liejun Zhong [a,*], Ming Li [a], Da-Lin Zhang [b]

[a] Horn Point Laboratory, University of Maryland Center for Environmental Science, P.O. Box 775, Cambridge, MD 21613, USA
[b] Department of Atmospheric and Oceanic Science, University of Maryland, College Park, MD 20742, USA

ARTICLE INFO

Article history:
Received 31 July 2009
Accepted 4 July 2010
Available online 16 July 2010

Keywords:
storm surge
hurricane
tropical cyclone
sensitivity analysis
Chesapeake Bay

ABSTRACT

With the increasing demand for accurate storm surge predictions in coastal regions, there is an urgent need to understand and quantify how the predictive skill of the hydrodynamic model is affected by various uncertainties in the atmospheric model forecasts for hurricanes. In this study, a series of numerical sensitivity experiments is conducted for the storm surge in a semi-enclosed Chesapeake Bay generated during the passage of Hurricane Isabel (2003). It is found that the predicted storm surge is sensitive to errors in predicting the hurricane's track, intensity and propagation speed. The surge height is more sensitive to the wind forcing in the upper Bay than in the lower Bay due to different response mechanisms in the two regions. Errors in the translation speed change the prediction of not only the surge height, but also its arriving time and duration of high water, whereas errors in the hurricane track and intensity mainly affect the model prediction on the surge height. In addition, the storm surge prediction is more sensitive to the spatial than temporal resolution of the predicted horizontal wind field.

1. Introduction

Storm surge induced by tropical cyclones (TCs) is one of the major threats to the life and property of coastal regions. On average, roughly 5 TCs every 3 years would strike the U.S. coastline, causing 50–100 casualties and billions dollars of property damage (http://www.nhc.noaa.gov/HAW2/english/basics.shtml). Thus, accurate prediction of storm surge has been listed as a high priority by the coastal disaster planning and mitigation agencies. For this reason, many numerical models have been developed to study storm surge (e.g., Flather et al., 1991; Verboom et al., 1992; Westerink et al., 1992; Hubbert and McInnes, 1999; Xie et al., 2004), and to predict its occurrence in an operational setting (e.g., Flather et al., 1991; Jelesnianski et al., 1992; Vested et al., 1992; Gerritsen et al., 1995).

The basic physics of storm surge is well understood. It is determined primarily by meteorological forcing, such as TC intensity, path, spatial and temporal scales, and topographic parameters including the width and slope of continental shelf, geometry and character of local coastal and shelf features (e.g., barrier islands, headlands, bays, sounds, inlets, marshes, channels, levees, and barriers). Thus, the predictive skill of any storm surge model depends critically on the input of TC winds and the representation of local bathymetric and topographic features. The latter requires adequate model grid resolutions, and high-resolution geographic data translated to model computational grids.

Despite the importance of the surface wind forcing, some storm surge models, e.g., the National Hurricane Center's (NHC) Sea, Lake and Overland Surges from Hurricanes (SLOSH) model, are still driven by parametric surface winds (Peng et al., 2004, 2006; Shen et al., 2006) that are estimated by assuming an idealized stationary, symmetric TC with the observed path, surface pressure drop, and radius of maximum wind (RMW), or by the planetary boundary layer (PBL) hurricane wind model (Scheffner and Fitzpatrick, 1997). Thus, its operational utility has been limited by its great sensitivity to errors in input parameters, such as the storm track, intensity and size (Rappaport et al., 2009). NOAA/Hurricane Research Division (HRD) has developed more accurate hurricane winds in real time (Powell et al., 1998; Houston et al., 1999) that have recently been used to drive storm surge models; these winds are based on all available surface wind observations from buoys, coastal-marine automated observation platforms, ships, and other surface facilities. However, the HRD surface winds are only available prior to landfall. Because of many uncertainties associated with surface winds and other model parameters, ensemble storm surge forecasts using ensemble meteorological forecasts due to different initial perturbations or different physics options have been proposed. Nevertheless, little

* Corresponding author. CSIRO Marine and Atmospheric Research, Underwood Avenue, Floreat, WA 6014, Australia.
E-mail address: Liejun.Zhong@csiro.au (L. Zhong).

0272-7714/$ – see front matter © 2010 Elsevier Ltd. All rights reserved.
doi:10.1016/j.ecss.2010.07.001

is understood about the impact of various uncertainties involved in the numerical prediction of storm surge.

Using the Holland (1980) parametric wind model for 10 idealized TCs passing over the Croatan-Albemarle-Pamlico Estuary System (CAPES), Peng et al. (2004) found that the storm surge and inundation over the eastern North Carolina are sensitive to TC's translation speed, RMW, minimum central pressure (MCP), and inflow angle. Later, Peng et al. (2006) examined how the above parameters affect sea-level rise and fall asymmetries. The work of Peng et al. (2004) focuses on the response of CAPES to passing hurricanes rather than the predictive skill of the storm surge model.

The purpose of the present study is to examine how various uncertainties in the atmospheric model forecasts of hurricanes affect the accuracy of storm surge prediction, using Chesapeake Bay as a study site. Semi-enclosed bays, such as Chesapeake Bay, have complex and intricate coastlines, which can either protect the large population centers they harbor, or render them particularly vulnerable to trap, amplify storm surges (Boicourt, 2005). The response of such a coastal system depends critically on the wind field and small differences in the relative positions of the storm track and the Bay's axis. Therefore, Chesapeake Bay is a coastal system well suited for conducting a stringent test of storm surge models. In this paper we carry out sensitivity analyses of the simulated storm surge to various predicted meteorological variables such as storm intensity, track and translation speed, and model spatial and temporal resolutions. Specifically, we use a regional coupled atmosphere-ocean model to study the storm surge in Chesapeake Bay during the passage of Hurricane Isabel (2003). The model reproduces reasonably well the storm surge and associated bay currents that are driven by high-resolution surface winds (see Li et al., 2006, 2007). Considering the growing demand for accurate storm surge prediction with the coupled models, we are motivated to investigate how errors in the predicted surface winds from the mesoscale hurricane-forecast models will propagate into the hydrodynamic models of coastal oceans, and how they affect the quality of the storm surge prediction.

The next section describes the model and its configuration. Section 3 presents the design of numerical experiments while Section 4 shows various sensitivity simulation results. Section 5 provides an error analysis of model predictions. Concluding remarks are given in the final section.

2. Model description and the control run

In this study, the two-dimensional version of a hydrodynamic model of Chesapeake Bay (Li et al., 2005; Zhong and Li, 2006; Zhong et al., 2008), based on the Regional Ocean Modeling System (ROMS) (Shchepetkin and McWilliams, 2005), is one-way coupled to the Penn State University – National Center for Atmospheric Research mesoscale model (i.e., MM5). A nested-grid (36/12/4 km) version of the MM5 was used in real-time daily forecast mode at the University of Maryland (UMD) to provide hurricane prediction (see http://www.atmos.umd.edu/~mm5 for more details). The MM5's initial and lateral boundary conditions were obtained from the National Center for Environmental Prediction regional analysis and forecasts, respectively. The outermost to innermost domains are centered at (85°W, 39°N), (94°W, 46°N) and (79°W, 45°N), with the grid dimensions of 73×97, 70×88, 85×103, respectively. The important model physics of the MM5 relevant to the hurricane prediction includes: (1) the latest version of the Kain and Fritsch (1993) convective scheme; (2) an explicit moisture scheme containing prognostic equations for cloud water (ice) and rainwater (snow) (Dudhia, 1989; Zhang, 1989); (3) a modified version of the Blackadar PBL scheme (Zhang and Anthes, 1982); (4) a simple radiative cooling scheme (Grell et al., 1995); and (5) a multi-layer soil model to predict land surface temperatures using the surface energy budget equation (Dudhia, 1989).

The MM5's hourly surface wind stress (SWS) at the finest resolution of 4 km for a period of 48-h prediction was used to drive the ROMS for Chesapeake Bay and its tributaries. As verified against various observations, the MM5 predicts reasonably well the trajectory and intensity of Hurricane Isabel as well as the other meteorological fields (Li et al., 2006). However, the surface winds at a mid-Bay station appear to be slightly overpredicted (see Fig. 1). Note that both the observed and predicted storms weaken with time after landfall, and move northwestward away from the Bay.

Chesapeake Bay is shallow in most places, but a deep paleo-channel running in the north-south direction dominates the bathymetry in the middle reaches of the main Bay (Fig. 2a). The ROMS domain covers the main stem of Chesapeake Bay, all major tributaries and a part of coastal ocean. An orthogonal curvilinear coordinate system is designed to follow the central channel and coastlines of the main stem (Fig. 2b). With a grid size of 80×120, the model has horizontal resolutions of about 1 km in the cross-channel direction and 2–3 km in the along-channel direction. The model bathymetry including elevation over adjacent land surfaces is extracted from the Coastal Relief Model data archived at NOAA's National Geophysical Data Center (NGDC). To simulate possible overland inundation caused by storm surges, we incorporate a simple wetting-and-drying scheme provided by the ROMS model (cf. Oey, 2005). The formulation is based upon the concept of a 'critical depth' (D_{crit}) criterion (cf. Zhang et al., 2004; Oey, 2005). As the model progresses, the total depth $(h+\eta)$ in each cell is compared to D_{crit}. If $(h+\eta) < D_{crit}$, a 'flux blocking' algorithm is

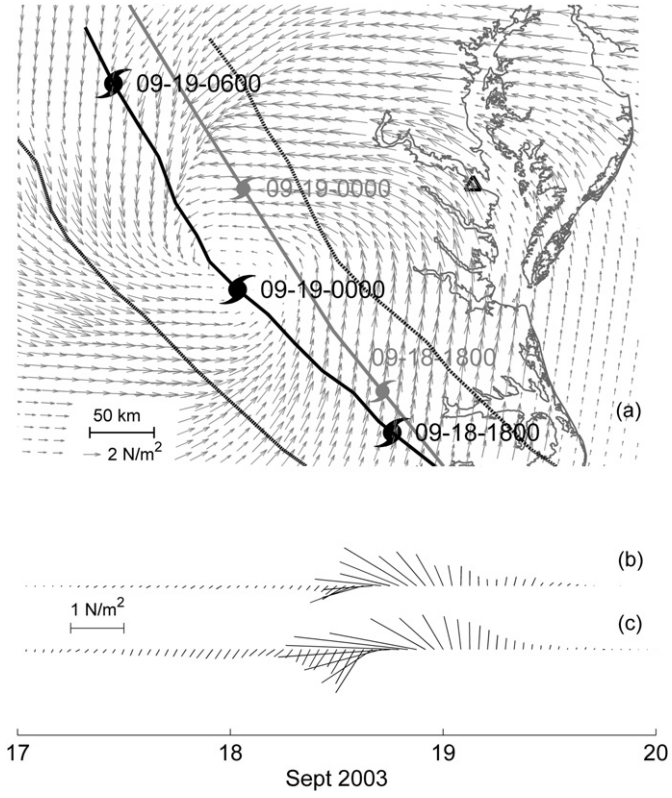

Fig. 1. (a) The MM5-predicted surface wind stress field at 0000 LST 19 September 2003, superposed with the predicted (dark solid) and observed (light solid) tracks of Hurricane Isabel, and two hypothetical tracks (dashed/dash-dotted on the west/east side of the predicted track). Time series comparison of (b) the observed winds and (c) the predicted winds during 0000 LST 17 and 0000 LST 20 September 2003 at a mid-Bay station Lewisetta [shown by a triangle in (a)].

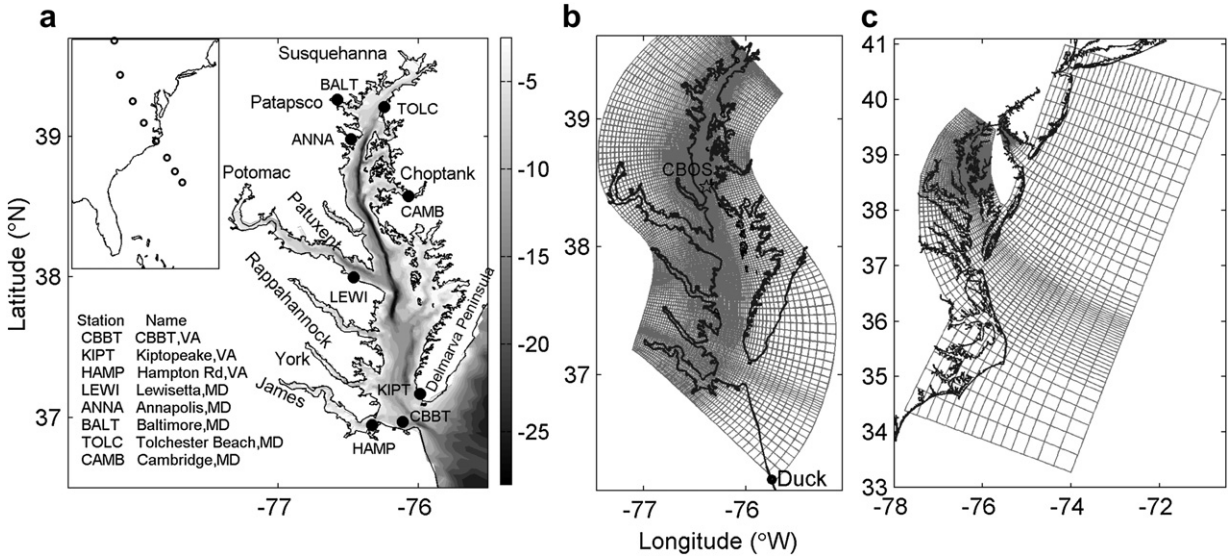

Fig. 2. (a) Bathymetry of Chesapeake Bay (shading scales are in meters) and location of the selected tidal-gauge stations (solid dots) used for the model-data comparison. The inset at the upper-left corner shows the geographic location of Chesapeake Bay in the Eastern U.S. and the track of Hurricane Isabel 2003; (b) and (c) two horizontal curvilinear coordinate systems used for the ROMS model. The star symbol in (b) marks the location of CBOS mid-Bay buoy station where wind stress predictions between the different model runs are compared. In (c), every 7th grid line is plotted in both along- and cross-bay directions.

imposed to prevent transport out of that cell. Water can flow into any cell at any time, but the water cannot flow out if the total depth is less than D_{crit}. Cells become rewet if water flows back from adjacent cells. In our application, we choose $D_{crit} = 0.2$ m. The frictional stress on the bottom boundary is parameterized as a quadratic function of the depth-averaged current with a constant drag coefficient of 0.0025.

External forcing for the ROMS model includes sea level at the open ocean boundary and freshwater inflows at river heads. Tidal elevation at the open boundary is decomposed into five major tidal constituents, M_2, S_2, N_2, K_1, O_1, using the harmonic constants linearly interpolated from the Oregon State University (OSU) global inverse tidal model TPXO.6.2 (Egbert and Erofeeva, 2002). These five constituents account for about 95% of total tidal variability in Chesapeake Bay (Browne and Fisher, 1988). Non-tidal coastal sea-level fluctuations are specified using detided sea-level records at the two tidal stations: Duck, North Carolina, and Kiptopeake, Virginia (see Fig. 2 for their locations). The latter is used because the Wachapreague station outside the Bay's mouth was out of order during the passage of Isabel. The constructed offshore sea-level elevation at the open boundary is demonstrated in Fig. 3. The open ocean boundary condition consists of a Chapman's condition for surface elevation and a Flather's condition for barotropic velocity. The model includes eight major tributaries: Susquehanna, Patapsco, Patuxent, Potomac, Rappahannock, York, James and Choptank. At the upstream boundary in each tributary, the incoming current is regulated by freshwater discharge rate, and the Chapman radiation condition is used to filter out the outgoing tidal waves (Zhong and Li, 2006).

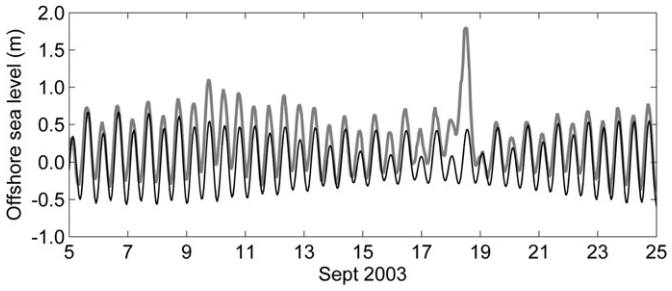

Fig. 3. Comparison of tidal (black) and total (gray) sea-level fluctuations at the offshore tidal station Duck, North Carolina (shown in Fig. 2b) between 0000 LST 5 and 0000 LST 25 September 2003, covering the passage of Hurricane Isabel.

As shown in Fig. 1, horizontal winds from Hurricane Isabel began to affect Chesapeake Bay on 17 September 2003. Therefore, our numerical experiments start integration from 16 September. To generate an initial condition, we run the model over a spin-up period (1 August–15 September). The predicted sea level and currents at the end of 15 September are then used as the initial conditions for the storm surge experiments. It should be noted that the predicted storm surges are insensitive to the initial conditions, but the inclusion of the spin-up period produces longer time series in sea level, allowing for accurate removal of tidal signals and more precise determination of storm surges. Fig. 4 shows that the model captures well the observed temporal evolution of sea-level elevations at 6 selected tidal-gauge stations. The root-mean-square (RMS) error averaged over 8 stations (see the locations in Fig. 2a) in the Bay is 0.12 m. The model's predictive skill, as defined by Warner et al. (2005) (see Section 5 for details), has a score of 0.97. The elevation dataset provided by NGDC has relatively coarse horizontal resolutions over land and may not provide accurate inundation predictions in certain local regions. Nevertheless, incorporating overland inundation improves the prediction of storm surges as the overflowing water is allowed to flood the adjacent land. By comparison, the previous model which did not consider inundation effects overpredicted the surge heights at tidal stations in Baltimore and Annapolis (Li et al., 2006). We name this model run as the control run (CTRL), which will be used as a base case to compare with other sensitivity experiments.

Most of the numerical experiments described in this paper are conducted using this limited-area model in which non-tidal sea-level fluctuations need to be prescribed at the open boundary. In order to test the sensitivity of storm surge predictions to the open boundary conditions and eliminate the need to specify non-tidal coastal sea-level fluctuations, we designed a large model domain covering the Middle Atlantic Bight, Chesapeake Bay and Delaware Bay. It extends from 34°N to 41°N with the offshore boundary located at about 1000-m isobath (see Fig. 2c). The model has a grid

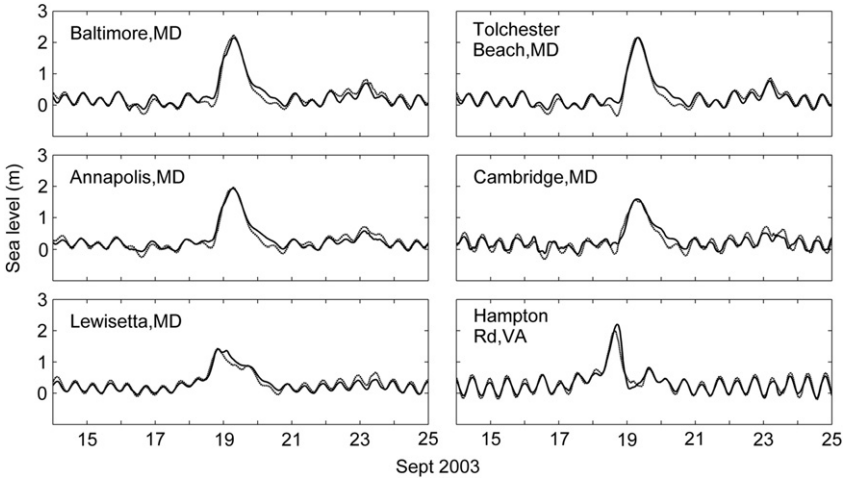

Fig. 4. Time series comparison of the control-predicted (slid) and observed (dashed) sea-level elevations at selected tidal-gauge stations (see Fig. 2a for locations) during the period of 0000 LST 14–0000 LST 25 September 2003.

size 600×360 in the along-shelf and cross-shelf directions, respectively. This model is configured in the same way as the limited-area model except that only tidal forcing is imposed at its offshore open boundary. With a larger model domain, the model is capable of simulating storm surges generated in the shelf and North Atlantic Ocean. For computational efficiency, we ran the large-domain model over a 12-day period between 10 and 22 September 2003.

3. Experimental design

A total of 13 numerical experiments, as summarized in Table 1, have been conducted to examine the sensitivity of storm surge prediction to possible uncertainties in atmospheric model forecasts for Hurricane Isabel (2003). Eleven of them are based on the limited-area model, each having one particular parameter different from CTRL in the coupled MM5–ROMS modeling system while holding all other variables the same. Two additional experiments are carried out in the big-domain model to examine the effects of offshore sea-level forcing on the storm surge predictions inside Chesapeake Bay. To facilitate the comparison of model results, we categorize the sensitivity runs into the following 5 groups.

The intensity, track and propagation speed of a storm are the most important parameters predicted by a hurricane model. Thus, we have conducted numerical experiments to examine how possible errors in predicting these hurricane parameters affect storm surge prediction in the semi-enclosed Chesapeake Bay. These "errors" could be caused by uncertainties in the MM5's initial and boundary conditions, grid resolutions, and model physics representations. In Group A, the CTRL surface wind field is shifted 100 km westward (WTRK) and eastward (ETRK), respectively, to examine the sensitivity of the storm surge to possible forecast errors on the hurricane track. Due to different roughness heights, there are some differences in SWS over land and water surfaces. These land–sea differences cannot be easily incorporated into the numerical experiments. Given that the horizontal scale of the storm is much larger than Chesapeake Bay, however, we expect that the Bay exerts minimal impact on the Hurricane's wind field. In Group B, the CTRL SWS is multiplied by a factor of 0.25 (WEAK) and 2.25 (STRG), respectively, to see how errors in predicting hurricane intensity affect the storm surge prediction in Chesapeake Bay. They are equivalent to a 50% decrease or increase in surface winds, respectively. In Group C, the propagation speed of the storm after the landfall (i.e., at 1700 LST 18 September 2003) is doubled (FAST) or halved (SLOW), respectively, to study to what extent the storm movement affects the magnitude of storm surge. This is achieved simply by shifting the two-dimensional surface-layer fields at the specified speeds. As summarized by Rappaport et al. (2009), the average errors in the NHC forecasts for storms hitting the U.S. coasts between 2000 and 2007 are 160 km for the storm track and 10 m s^{-1} for the storm intensity due to the lack of observations over the vast tropical oceans and deficiencies in hurricane models. Therefore, the variations of the above storm-related parameters are within the error ranges of hurricane models.

In the second set of numerical experiments, we examine how the temporal and spatial resolutions of surface wind predictions in the atmospheric model affect the prediction of storm surges in the hydrodynamic model. In Group D three sensitivity simulations are conducted using the surface winds provided by the MM5 at the following intervals: (1) 6 hourly intervals at the 4-km resolution (6HR); (2) hourly intervals at 12-km resolution (12KM); and (3) hourly intervals at 36-km resolution (36KM). Because of the use of the two-way interactive nested grids, the 12- and 36-km resolution wind data in the MM5 are obtained by feeding back finer-resolution information (Zhang et al., 1986). (Note that the ROMS' spatial resolutions are not altered.) So, little difference among the CTRL, 12KM, and 36KM simulations could be seen in terms of the timing and location of the predicted storm, except for its mesoscale flow structures and central (point) intensity. One can see that the latter

Table 1
Experimental design.

Group index	Experiment	Remarks
A	WTRK	Displace the hurricane track 100 km westward away from the Bay
	ETRK	Displace the hurricane track 100 km eastward towards the Bay
	BIGE	Big-domain model run with the hurricane track shifted as in ETRK
B	WEAK	Decrease the control wind speed by 50%
	STRG	Increase the control wind speed by 50%
C	SLOW	Halve the hurricane translation speed
	FAST	Double the hurricane translation speed
D	6HR	Six-hourly, 4-km resolution surface wind
	12KM	Hourly, 12-km resolution surface wind
	36KM	Hourly, 36-km resolution surface wind
E	NTID	Exclude non-tidal oscillations at the open boundary
	NWND	Exclude wind forcing at the water surface
	BIGC	Big-domain model run with the control wind field

two sensitivity simulations are more meaningful than those using the surface winds obtained from meteorological model forecasts with two different resolutions. As expected, horizontal winds over Chesapeake Bay tends to be poorly resolved at coarser spatial resolutions; for example, only 9 data points in the 36-km resolution domain covers the Bay in the longitudinal direction.

Fig. 5 compares 3-day time series of SWS at the CBOS (Chesapeake Bay Observing System) mid-Bay buoy station between the CTRL and sensitivity experiments (the wind anemometer was damaged during the storm's passage so that no wind data were available for comparison with the model results). Clearly, changing any of the parameters listed in Table 1 could produce notable differences in the SWS time series from the CTRL one. In particular, if the hurricane track were predicted 100 km eastward closer to the Bay (ETRK), the SWS at all the stations would increase substantially. In fact, the SWS at the CBOS station (Fig. 5c) experiences the largest increase in magnitude among all the sensitivity simulations (cf. Fig. 5a–j). If the storm translation speed were predicted to be slower (SLOW), the life span of the storm or the time window for the passing storm to produce significant storm surge would be significantly extended (cf. Fig. 5a and f); the opposite is true with the faster migration speed (FAST, see Fig. 5g). When the surface wind data is sampled at a lower frequency (i.e., 6HR), some extreme values or details may be missed or lost (cf. Fig. 5a and h). (Note the hourly plots, linearly interpolated from the 6-hourly data, are shown in Fig. 5h to facilitate the simulation inter-comparisons.) For example, the average westward SWS from 1500 LST 18 to 0000 LST 19 September in 6HR is much weaker than that in CTRL. When the surface wind data at coarser spatial resolutions (i.e., in 12KM and 36KM) are used, the SWS over the narrow Bay's surface tends to become larger due to the "averaging" influence of the SWS values at the neighboring land points (cf. Fig. 5a, i and j). Clearly, all of the above differences in SWS would produce changes in storm surges when they are used to drive any oceanic model, as will be seen in the next section.

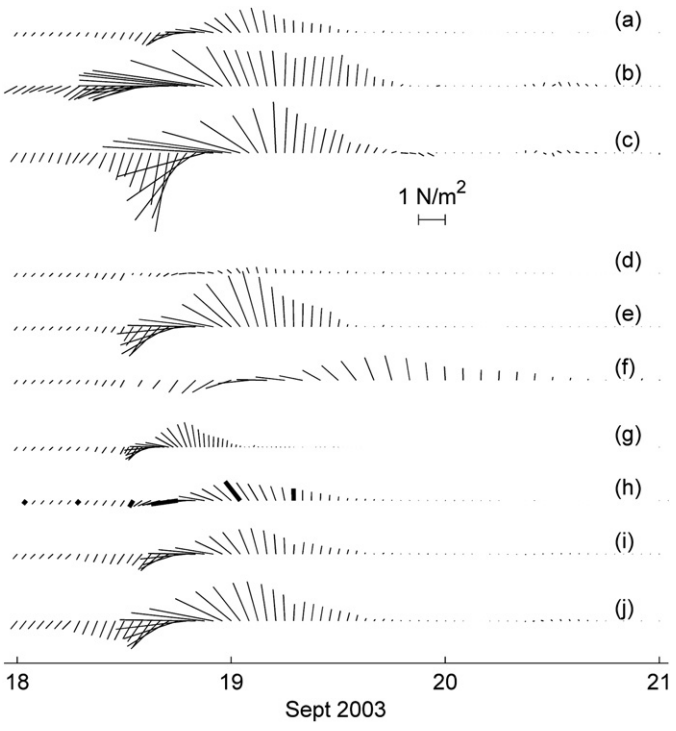

Fig. 5. Time series comparison of the surface wind stress at the CBOS mid-Bay station (its location shown by a triangle in Fig. 2b) from (a) CTRL (control); (b) WTRK (westward track); (c) ETRK (eastward track); (d) WEAK (50% decrease in intensity); (e) STRG (50% increase in intensity); (f) SLOW (halved moving speed); (g) FAST (doubled moving speed); (h) 6HR (6-hourly data; thick solid lines are from 6-hourly data and thin solid lines are from linearly interpolated data); (i) 12KM (12-km resolution data); and (j) 36KM (36-km resolution data).

Our previous simulations have shown that the inverse barometer effect was small during the passage of Hurricane Isabel (Li et al., 2006, 2007). As shown in Fig. 1, the center of Isabel was over 200 km away from Chesapeake Bay. The central pressure varied from 957 to 987 mb between 17 and 19 September with a maximum pressure drop of 56 mb. The RMW was about 85 km (Shen et al., 2006). Using an empirical vortex model, we estimate the pressure drop $\Delta p = -56[1 - e^{-(85/r)^{1.9}}]$ (see Peng et al., 2006; where r is the distance from the storm's center) to be 10 mb at $r = 200$ km and 5 mb for $r = 300$ km. This would translate to a sea-level rise of 10 cm and 5 cm, respectively, which are much smaller than those sea-level changes found in the model runs. Hence, the inverse barometer effect will not be considered in this paper.

As a semi-enclosed Bay, Chesapeake Bay is subjected to both local and remote wind forcing (Garvine, 1985). In Group E, we conduct two model runs to compare the relative roles of local wind forcing versus remote wind forcing in generating storm surges during the passage of Isabel. In NTID, non-tidal seal-level fluctuations are turned off at the open boundary so that the storm surge generated in the open shelf is not allowed to propagate into the Bay. However, the storm surge can still be generated by local winds acting on the Bay's surface. In NWND, both tidal and non-tidal sea-level fluctuations are imposed at the open boundary whereas the local wind forcing over the Bay's surface is switched off. In this case, the coastal storm surge is allowed to propagate into the Bay but the local wind setup inside the Bay is suppressed.

The above sensitivity experiments are based on the limited-area model in which subtidal sea-level variations on the coastal open boundary must be specified. While the limited-area model allows for high-resolution predictions inside the semi-enclosed Bay, the requirement for the open boundary conditions makes it unfeasible for making storm surge forecasts. Therefore, we conduct two additional runs (BIGE in Group A and BIGC in Group E in Table 1) using the big-domain model, in which storm surges in the adjacent Atlantic Ocean are directly simulated. These model runs provide sea-level forecasts which can be used to specify the open boundary condition in the limited-area model. We shall show later that BIGC and BIGE produce very similar predictions of storm surges as their counterpart runs CTRL and ETRK, respectively. It follows that results from Group A sensitivity experiments do not depend on the specification of the open boundary condition in the limited-area model.

The model predicts sea-level fluctuations which contain both storm surges and tides. To focus on the storm surge prediction, we remove tidal oscillations in the sea-level time series using the harmonics analysis method (see Zhong and Li, 2006) for the numerical experiments based on the limited-area model. Since the time series obtained from the big-domain model are not long enough for the harmonics analysis, an additional run is conducted to simulate tides which are then subtracted from the total sea-level heights produced from BIGC and BIGE. It is worth pointing out that both the large-domain and limited-area models produce accurate predictions of tidal heights inside the Chesapeake Bay.

4. Results

In this section, we present the sensitivity of the simulated storm surge to hurricane track (Group A), intensity (Group B), translation speed (Group C), open boundary condition and local wind forcing (Group D), and temporal and spatial grid resolutions (Group E). Their differences in the simulated storm surges will be compared to

both the CTRL-predictions and observations. For this purpose, a total of 8 tidal-gauge stations, given in Fig. 2a, are selected to characterize the predicted storm surges in the lower Bay [i.e., CBBT, Kiptopeake (KIPT), and Hampton Road (HAMP)], the middle Bay [i.e., Lewisetta (LEWI) and Cambridge (CAMB)], and the upper Bay [i.e., Annapolis (ANNA), Baltimore (BALT), and Tolchester (TOLC)], respectively.

4.1. Sensitivity to hurricane track (Group A)

Hurricane Isabel (2003) was observed to pass on the west side of Chesapeake Bay, while the CTRL track is located farther to the west of the observed (Fig. 1a). Shifting the CTRL track 100 km to its east (ETRK), i.e., closer to the Bay, produces much stronger winds, particularly prior to landfall, as shown in Fig. 5c. A naive visual comparison of storm tracks in Fig. 1a would suggest that the ETRK track is as close to the observed track as the CTRL track. However, in terms of storm surge generation inside the Bay, the most critical period is the first 6 h after the hurricane's landfall (i.e. before 0000 LST 19 September) when the predicted track in CTRL is very close to the observed track. This explains why CTRL provides accurate storm surge predictions. In contrast, the strong southward winds in ETRK generate large sea-level depression in the upper and mid-Bay prior to the landfall (Fig. 6). For instance, the sea-level depression at Tolchester Beach reaches over 2 m before the surge. In contrast, the sea level at Hampton Road changes from a surge height of 3 m to a depression of 1 m during the passage of the storm. Before the storm's landfall, a large sea-level slope is generated between the head and mouth of the Bay. While the southward winds acting on the Bay's surface causes the sea level to drop in the upper Bay, the southward wind blowing over the adjacent shelf produces onshore Ekman flux, leading to higher levels in the lower Bay.

Similar sea-level depression could also be seen from the observations, but at much smaller magnitudes, because of the weaker southward winds and shorter duration than those in ETRK. Fig. 5 shows that the maximum (southward) SWSs from the CTRL and ETRK on September 18 are 0.5 and 3.0 N m^{-2} at the CBOS mid-Bay station, respectively, with a variation of 6 times in magnitude. Clearly, the longer the southward winds are sustained, the stronger the sea-level depression (rise) near the Bay head (mouth) would occur. The depression in the northern Bay is so strong that it counteracts with the subsequent sea-level rebound after the wind is switched to the northward direction. As a result, the surge heights in the middle and upper Bay in ETRK are weaker than those in CTRL (Fig. 6), even though the northward SWS is much stronger than the CTRL (see Fig. 5a and c). This suggests that the passage of an intense TC near the Bay does not imply the occurrence of correspondingly intense storm surges, because wind directional shifts along the Bay may compensate for the water mass transport to the upper Bay. In this sense, it is desirable to predict reasonably well the TC track and its RMW with respect to the Bay's orientation.

The predicted arrival time of the peak surge in ETRK is delayed in the upper Bay (see Fig. 6) because the maximum northward wind occurs a few hours later than that in CTRL (Fig. 5a and c). The enhanced northward winds in ETRK produce a 1-m post-surge depression in the lower Bay, e.g., at Hampton Road. While the northward winds blowing over the Bay's surface drive water towards the Bay's head, the northward winds blowing over the shelf drive an offshore Ekman flux, causing the sea level to drop at the Bay's mouth.

When the track is shifted 100 km to the west of the CTRL one (WTRK), i.e., even farther away from the Bay, the surface winds experienced by the Bay water are likely weaker than those in CTRL. However, due to the land–sea difference in the roughness height, SWS at the CBOS mid-Bay station is larger in WTRK than in CTRL. In general, the simulated storm surges in WTRK are slightly larger than the CTRL-predicted (Fig. 6) at the mid-Bay and upper Bay stations but slightly lower at the lower Bay stations. The longer sustained northward wind in WTRK makes longer duration of higher water level in the upper Bay (i.e., Baltimore, Tolchester and Annapolis in Fig. 6) than that in CTRL.

In the above two experiments, we prescribe the observed non-tidal sea levels at the offshore boundary of the limited-area model. It is quite possible that the offshore boundary conditions could be changed if the storm track is shifted. To address this concern, we conduct another run (BIGE) using the big-domain model but with the wind field identical to that in ETRK. This model simulates the storm surges generated in the adjacent coastal ocean. As shown in Fig. 6, the BIGE-predicted storm surge is very similar to that obtained from ETRK: both runs produce large sea-level depression in the middle and upper Bay prior to the landfall, sea-level rise and fall at the Bay's mouth during the passage of the storm. The close agreements between BIGE and ETRK suggest that it is reasonable to use the prescribed non-tidal sea level at the offshore open boundary of the limited-area model in the sensitivity-analysis experiments.

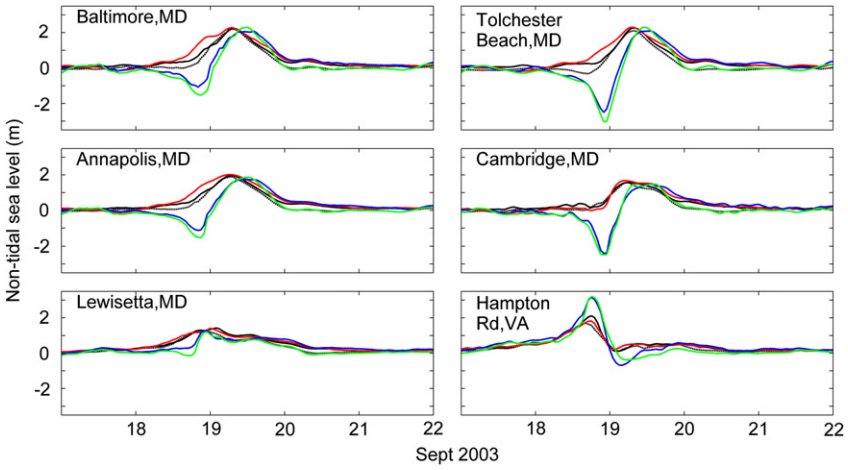

Fig. 6. Comparison of subtidal sea-level elevations from OBS (observed; dashed black), and CTRL (control run; solid black), and from Group A sensitivity experiments: WTRK (westward track; red), ETRK (eastward track; blue), and BIGE (big-domain model run with hurricane track shifted eastward; green).

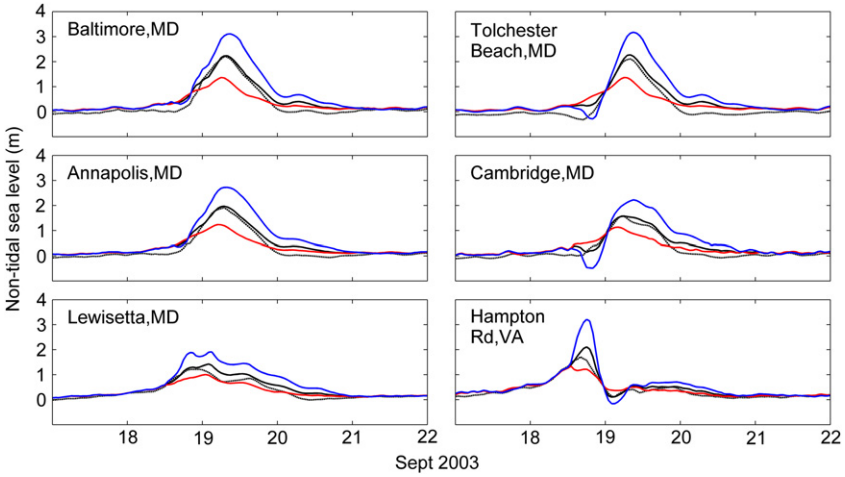

Fig. 7. As in Fig. 6, but for Group B sensitivity simulations: WEAK (50% decrease in intensity; red) and STRG (50% increase in intensity; blue).

4.2. Sensitivity to hurricane intensity (Group B)

Fig. 7 shows the temporal evolutions of the predicted storm surges for different hurricane intensities. Increasing the storm intensity by 50% (i.e. SWS multiplied by 2.25) leads to 30–55% increases in storm surge, i.e., between the STRG and CTRL. Similarly, about 15–40% decreases in surge height occur when the hurricane intensity is reduced by 50% (i.e. SWS multiplied by 0.25). The magnitudes of the storm surge heights among the observations, CTRL, WEAK and STRG are not linearly proportional to their corresponding SWS. While the surge heights among the CTRL, WEAK and STRG runs show large differences at some stations (e.g., Baltimore, Tochester and Hampton), the differences at the other stations are relatively small (e.g., Cambridge and Lewisetta). In STRG, sea-level depression prior to the landfall is evident at some upper Bay stations (i.e., Tolchester and Cambridge). Hurricane intensity also changes duration of high water level and its variation is much larger in the middle and upper Bay than in the lower Bay due to the phase lag between freely propagating surge originated offshore and forced surge driven by local winds.

4.3. Sensitivity to hurricane translation speed (Group C)

Translation speed of the storm is another important parameter predicted by hurricane models. The time series of SWS at the CBOS station, given in Fig. 5f and g, indicates that slowing down (speeding up) the hurricane movement extends (shortens) the duration of surface forcing on the storm surge in the Bay. In particular, varying the translation speed alters not only the arriving time of the surge peak but also the duration of the higher water level (defined as a surge height of greater than 1 m), especially at stations in the upper Bay (see Fig. 8).

Fig. 9 quantifies differences in the storm surge height, the arriving time of the peak and the duration of high water level relative to the CTRL-run. Slowing down the translation speed (SLOW) leads to increases in the peak surge height at middle Bay stations (Hampton, Lewisetta, Cambridge and Annapolis) but small decreases in other lower and upper Bay stations (CBBT, Kiptopeake and Tolchester). By comparison, increasing the translation speed (FAST) produces much lower sea levels than those in CTRL at the upper Bay stations, e.g., close to 1 m lower at Baltimore, Tolchester and Annapolis, but moderate changes at the lower Bay stations (see Fig. 9a). Because the life span of the FAST hurricane is short, the surface winds do not have enough time to set up sea level in the upper Bay even though its intensity is the same as the CTRL one. This finding is consistent with the results obtained from the storm surge study in Tampa Bay (Weisberg and Zheng, 2006).

It is apparent from Fig. 9b that the translation speed also affects the phase of storm surge since it determines the time the local maximum surface wind arrives. It is reasonable to expect that

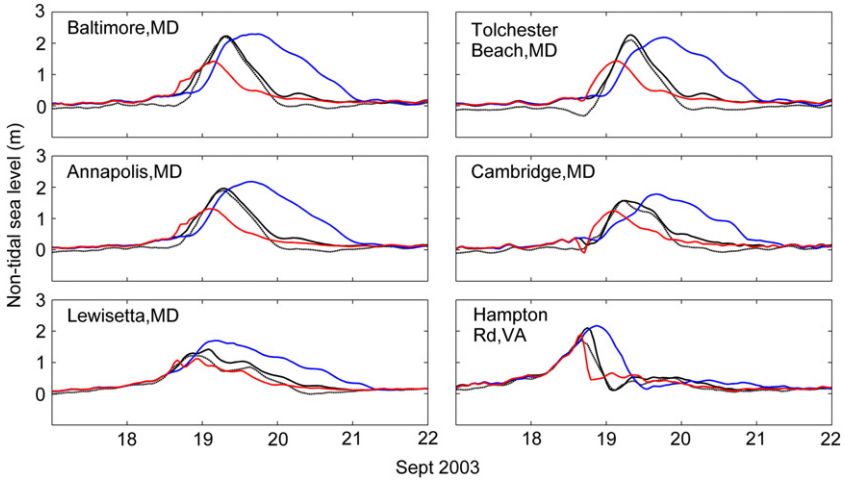

Fig. 8. As in Fig. 6, but for Group C sensitivity simulations: SLOW (halved moving speed; blue), and FAST (doubled moving speed; red).

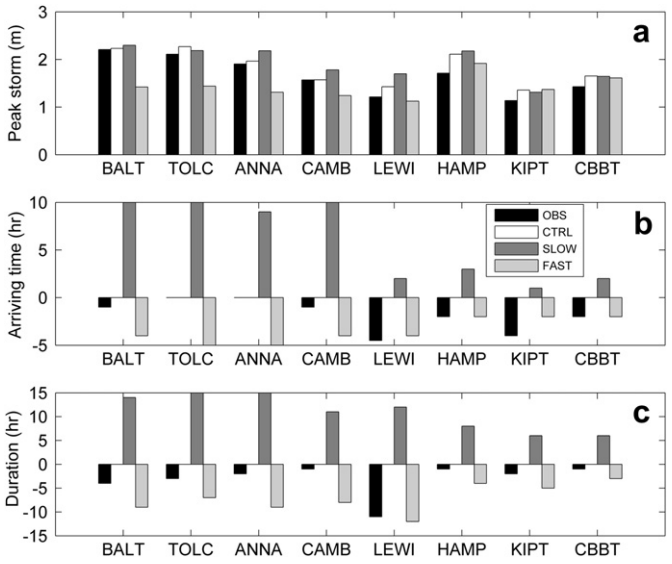

Fig. 9. Comparison of (a) peak storm surges; (b) their arriving times; and (c) durations of the higher-than 1-m water level from OBS (observed; dark black), and CTRL (control; blank), with Group C sensitivity simulations: SLOW (halved moving speed; light black) and FAST (doubled moving speed; gray) at selected tidal-gauge stations. Note that the arrival timings in (b) and the high-water durations in (c) are relative to the control-simulated.

a slower moving storm would generate the peak surge at a later time. For example, since the CTRL translation speed is slightly slower than the observed (Fig. 1), its peak surge lags behind the observed by 2–4 h at the lower Bay stations but it is in good agreement with the observed at the upper Bay stations. When the translation speed in SLOW is further reduced from the CTRL, the time lag of the peak surge increases to about 5 h in the lower Bay and more than 5 h in the middle and upper Bay. When the translation speed is doubled (i.e., FAST), however, the peak of storm surge arrives at the upper Bay stations ahead of the observed by 3–5 h. In contrast, the arriving time in FAST agrees well with the observed at the lower Bay stations except at Kiptopeke where it lags behind for about 3 h.

The effects of changing the translation speed on duration of the high water level (i.e., greater than 1 m) relative to the observed at individual stations are given in Fig. 9c, showing that the CTRL duration is about 2–4 h longer than the observed at all the tidal stations, except at the mid-Bay station Lewisetta. Doubling the translation speed (FAST) produces 3–9 h shorter high-water durations than those in the CTRL run. This is understandable because of the reduced duration of surface wind forcing. The FAST duration is shorter than the observed in most of the mid- and upper Bay stations (except at Lewisetta) but is indistinguishable from the observed at the lower Bay stations.

In contrast, the duration of high-water level is much longer in SLOW than CTRL, e.g., about 5–8 h in the lower Bay and 15 hours in the upper Bay (Fig. 9c). Such pronounced differences between the upper and lower Bay stations are attributable to the analysis that the storm surge in the upper Bay is driven more by local (northward) surface winds than that in the lower Bay, as will be discussed in Group E analysis.

4.4. Sensitivity to the resolutions of surface winds (Group D)

Since the data resolutions exhibit little differences in the timing and location of the storm, as mentioned before, the temporal characteristics of the simulated storm surge in this group should be similar to those in the CTRL, including the arriving time of the surge peak. So we only need to compare different peak magnitudes of the simulated surge to those using different resolutions of surface winds. It is evident from Fig. 10 that the temporal resolution of the wind field affects the prediction of storm surge heights, particularly in the lower Bay region. The height differences between CTRL and 6HR are in the range of 0.3–0.6 m at CBBT, KIPT and HAMP but are less than 0.1 m in the mid- and upper Bay. A comparison of SWS between 6HR and CTRL in Fig. 5a and h reveals that the 6HR run underestimates the pre-landfall southward wind and does not capture the rapid switching from the southwestward to northwestward wind around the landfall. Wind forcing during this period is crucial to the sea-level setup in the lower Bay. Consequently, the 6HR run predicts significantly weaker surge heights than CTRL at the three lower Bay stations (HAMP, KIPT and CBBT). By comparison, the post-landfall northward wind, which is the dominant force driving the storm surges in the middle and upper Bay, is reasonably resolved in 6HR. This result demonstrates the need to resolve the rapid transition from the southward to northward winds during the passage of the storm. For a faster moving storm, it is even more important to have high temporal resolution outputs from hurricane models.

The spatial resolution of surface winds affects the storm surge prediction in a different way. When its spatial resolution becomes coarse, SWS on the water surface may become larger due to the "averaging" influence of the SWS values at the neighboring land points and thus may produce higher storm surges. The 12-km resolution surface winds (i.e., 12KM run) produce similar storm surges to the 4-km winds (i.e., CTRL) (see Fig. 10). A comparison between Fig. 5a and i shows that the 12KM SWS at the mid-Bay CBOS station is very similar to that in CTRL. However, the 36KM SWS is considerably stronger than the CTRL SWS (cf. Fig. 5a and j) due to the larger "averaging" influence from the neighboring land points. While the strong post-landfall northward wind would drive larger storm surge, its effect is somewhat negated by the sea-level depression generated by the strong pre-landfall southward wind. The net effect is that the peak surge height in the 36KM run is only moderately higher (less than 0.2 m) than that in the CTRL run. As the Bay's width varies from 40 km in the lower Bay to 10 km in the upper Bay, the "averaging" influence becomes greater in the upper Bay and hence larger difference of peak surge between 36KM and CTRL is seen in the upper Bay than in the middle and lower Bay (Fig. 10).

4.5. Sensitivity to open boundary condition and local wind forcing (Group E)

We now examine the relative contributions of local and remote wind forcing to the storm surges in Chesapeake Bay. Note that by

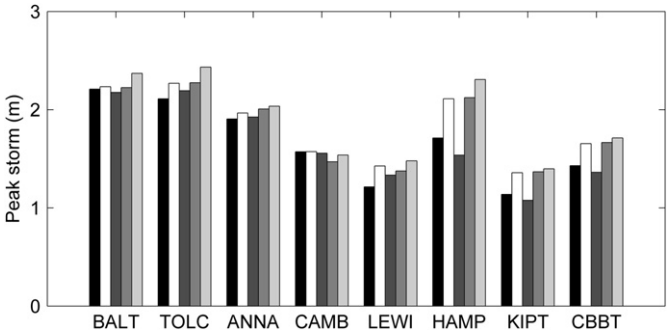

Fig. 10. Comparison of peak storm surges in Group D sensitivity simulations at selected stations. The bars at each station show the results in the order of OBS, CTRL, 6HR (6-hourly data), 12KM (12-km resolution data), and 36KM (36-km resolution data).

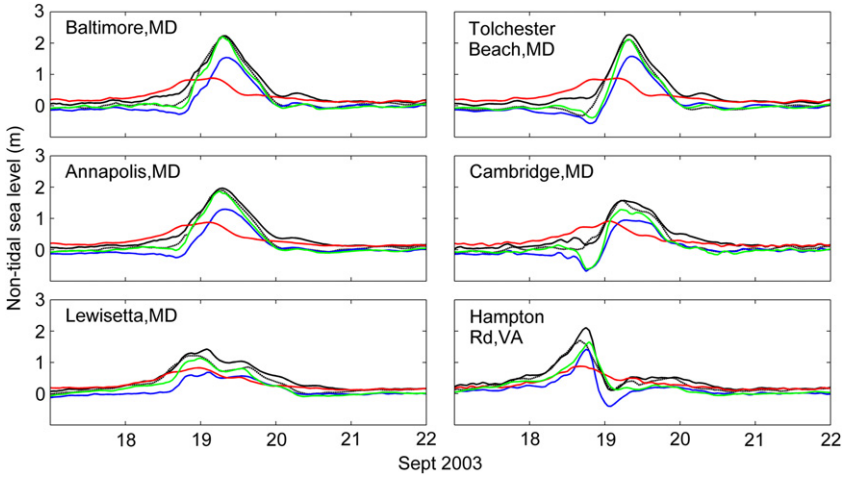

Fig. 11. Time series comparison of the subtidal sea-level elevations from OBS (observed; dashed), and CTRL (control; black solid), with Group E sensitivity simulations: NTID (no incoming coastal storm surge; blue), NWND (no local wind forcing; red) and BIGC (big-domain model run with the control wind fields; green).

turning off the offshore non-tidal sea-level fluctuations in NTID, we exclude the storm surges generated in the adjacent ocean, whereas by turning off the local wind forcing in NWND, we suppress the wind setup in the Bay.

Chesapeake Bay responds differently to the remote and local wind forcing. In run NWND, sea-level changes driven by the offshore sea-level setup show similar temporal evolution inside the Bay (Fig. 11). In fact, the peak surge heights obtained from NWND are nearly identical at all stations (Fig. 12a). The coastal surges propagate into the Bay as long waves and experience little dissipation or amplification (Zhong et al., 2008), although storm surges may experience significant amplifications in certain shallow estuaries, as demonstrated by Chen et al. (2008). In contrast, the local wind forcing drives large sea-level slope between the lower and upper Bay. In run NTID, the southward wind prior to the landfall produces sea-level depression in the upper Bay (e.g., Baltimore and Tolchester Beach) but sea-level rise in the lower Bay (e.g., Hampton Road), as shown in Fig. 11. The strong westward wind blowing at the landfall further raises the sea level in the lower Bay. After the landfall, the northward wind pushes water towards the upper Bay while lowering the sea level in the lower Bay. Fig. 12a shows that the local wind produces significantly larger surges in the upper Bay than in the lower Bay.

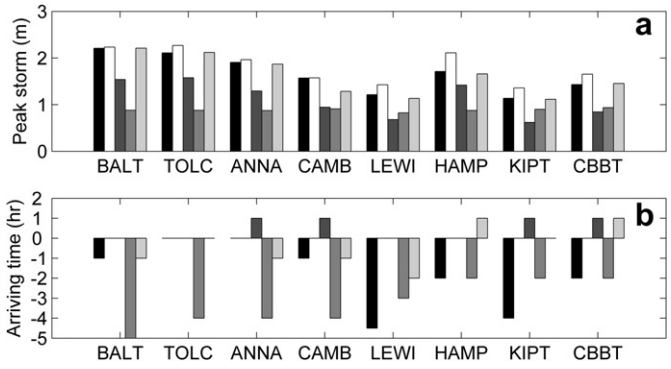

Fig. 12. Comparison of (a) peak storm surges, and (b) their arriving times from OBS (observed), and CTRL (control), with Group E sensitivity simulations at selected stations. The bars at each station show the results in the order of OBS, CTRL, NTID (no incoming coastal storm surge), NWND (no local wind forcing) and BIGC (big-domain model run with the control wind fields). Note that the arrival timing in (b) is relative to the control-simulated.

Neither local nor remote wind forcing alone can generate peak surge as large as that in CTRL (Figs. 11 and 12a), indicating that both are important in driving storm surges in Chesapeake Bay. However, their relative importance is different in different parts of the Bay. In the lower and mid-Bay stations (CBBT to Cambridge except Hampton Road), the incoming coastal surge and local wind forcing make nearly equal contributions to the surge height, while in the upper Bay local wind forcing generates significantly higher peak surge than incoming coastal surge (see Fig. 12a). Thus, the post-landfall local northward winds are especially important in generating sea-level setup and storm surges in the narrow and enclosed upper Bay. This point can be made clearer if we examine the arrival times of the peak surge in NWND and NTID; they are close to those in the CTRL-simulated at the lower and middle Bay stations, such as CBBT, Kiptopeake and Hampton Road (Fig. 12b). However, only the NTID-predicted peak surge synchronizes with the CTRL-predicted in the upper Bay whereas NWND-predicted peak surge arrives 4–5 h earlier. This finding is consistent with that of Shen et al. (2006). The CTRL-predicted storm surge can be regarded as the superimposition of NTID and NWND solutions because of the weak nonlinear interaction between the free and forced surges.

As discussed earlier, the non-tidal sea-level fluctuations at the offshore open boundary need to be prescribed in the limited-area model, but these boundary conditions will not be available in an operational setting. One way to circumvent this problem is to run a large-domain model that can directly simulate storm surges generated in the adjacent coastal ocean. Figs. 11 and 12 compare the BIGC to CTRL run, showing that BIGC provides reasonable predictions of storm surges inside the Bay. The outputs from this large-domain model can then used to prescribe the open boundary conditions for the limited-area ocean model.

5. Error analysis

In the preceding section, we examined storm surge responses to uncertainties in the MM5 such as the hurricane track, intensity and translation speed. To quantify the skill of the hydrodynamic model in predicting the storm surges, we compute the following statistical measures: the root-mean-square (rms) error

$$\mathrm{rms} = \left\{ \frac{1}{N} \sum_{i=1}^{N} (\eta_{\mathrm{mod}} - \eta_{\mathrm{obs}})^2 \right\}^{1/2}, \tag{1}$$

and the relative average error (E)

$$E = 100\% \frac{\sum_{i=1}^{N}(\eta_{\mathrm{mod}} - \eta_{\mathrm{obs}})^2}{\sum_{i=1}^{N}\left(|\eta_{\mathrm{mod}} - \overline{\eta}_{\mathrm{obs}}|^2 + |\eta_{\mathrm{obs}} - \overline{\eta}_{\mathrm{obs}}|^2\right)}, \quad (2)$$

where η represents the sea-level time series, $\overline{\eta}$ is its time mean while subscripts "mod" and "obs" denote the model results and observations, respectively. The correlation coefficient is calculated by

$$r = \frac{\sum_{i=1}^{N}(\eta_{\mathrm{mod}} - \overline{\eta}_{\mathrm{mod}})(\eta_{\mathrm{obs}} - \overline{\eta}_{\mathrm{obs}})}{\left[\sum_{i=1}^{N}(\eta_{\mathrm{mod}} - \overline{\eta}_{\mathrm{mod}})^2 \sum_{i=1}^{N}(\eta_{\mathrm{obs}} - \overline{\eta}_{\mathrm{obs}})^2\right]^{1/2}}, \quad (3)$$

following Spitz and Klinck (1998). We also examine the model skill as defined by Warner et al. (2005) in their simulations of the Hudson River estuary,

$$\mathrm{Skill} = 1 - \frac{\sum_{i=1}^{N}|\eta_{\mathrm{mod}} - \eta_{\mathrm{obs}}|^2}{\sum_{i=1}^{N}(|\eta_{\mathrm{mod}} - \overline{\eta}_{\mathrm{obs}}| + |\eta_{\mathrm{obs}} - \overline{\eta}_{\mathrm{obs}}|)^2}. \quad (4)$$

Perfect agreement between the model results and observations yields a skill of 1.0 whereas complete disagreement yields a skill of 0.

The time window selected for the statistical analyses is between 17 and 22 September 2003, a 5-day period covering the pre-landfall wind setup, Isabel's passage over Chesapeake Bay region and the post-landfall adjustment. In order to focus on the storm surge predictions, tidal signals are removed from the sea-level data using the harmonic analysis method (Zhong and Li, 2006). It should be noted that these statistical measures provide a skill assessment for the whole time series whereas the previous comparisons on the maximum surge height, arrival time and duration of high water level provide a different set of model assessment metrics.

The statistical analyses for the 14 model runs are summarized in Table 2. We first look at the sensitivity to hurricane track in Group A. The statistical errors in ETRK and BIGE are quite close since they generate very similar storm surge predictions. Their rms and E at the 8 stations are significantly larger than those in WTRK but r and skill are smaller. This implies that ETRK/BIGE performs worse than WTRK. Although the observed hurricane track lies between the CTRL and ETRK tracks, rms and E in ETRK/BIGE are considerably larger than in the CTRL run. The poor performance of ETRK/BIGE is caused by their overprediction of southward winds prior to landfall. As discussed in Section 4, the large southward wind before 0000 LST 19 September in ETRK/BIGE causes unrealistic sea-level depression in the upper Bay and sea-level surge in the lower Bay.

In Group B, the performance of the WEAK run is generally comparable to that of the CTRL run, though differing in different parts of the Bay. WEAK performs slightly better than CTRL in the lower Bay (i.e., smaller rms and E, and larger r and skill) but slightly worse in the upper Bay. SWS in the CTRL run is higher than the observed (cf. Fig. 1b and c) and even higher than in STRG (cf. Fig. 5a and e). Consequently, the predictive skill is the lowest in STRG with the largest rms and E among the Group B runs.

The analyses among the Group A and B runs show that uncertainties in hurricane track and intensity have little impact on the phase prediction of storm surge, as shown by high values of r across the board. The correlation coefficient r exceeds 0.9 at most stations in CTRL, WTRK, STRG and WEAK. But r is smaller in the ETRK/BIGE runs because they predict a strong pre-landfall sea-level depression which is absent in the observed and other runs. In contrast, the uncertainty in the storm translation speed changes the surge phase, as revealed from runs in Group C. The

Table 2
Statistical analyses of storm surge predictions from all model runs. Detided sea-level time series at 8 tidal stations are used in the analyses; rms (cm) denotes the root-mean-square error, E (%) the relative average error, r the correlation coefficient, and s the skill parameter.

		CTRL	Group A			Group B		Group C		Group D			Group E		
			WTRK	ETRK	BIGE	WEAK	STRG	SLOW	FAST	6HR	12KM	36KM	NTID	NWND	BIGC
BALT	rms	18.9	32.8	47.6	58.5	31.6	45.2	74.5	36.5	19.3	18.7	22.7	27.6	48.2	9.7
	E	5.0	13.0	26.7	38.0	20.4	18.5	57.0	26.4	5.4	4.8	6.2	13.2	54.3	1.3
	r	0.98	0.94	0.74	0.67	0.94	0.97	0.62	0.84	0.98	0.98	0.98	0.97	0.69	0.99
	s	0.98	0.94	0.85	0.79	0.89	0.91	0.71	0.85	0.97	0.98	0.97	0.93	0.64	0.99
TOLC	rms	24.9	36.1	72.2	83.0	33.8	49.3	78.0	38.3	25.1	22.6	26.4	25.0	51.4	13.8
	E	9.2	17.0	48.9	60.4	24.5	22.6	68.9	30.3	9.6	7.4	8.7	10.9	64.6	2.9
	r	0.98	0.94	0.54	0.48	0.91	0.95	0.55	0.81	0.98	0.98	0.96	0.94	0.58	0.98
	s	0.96	0.92	0.71	0.65	0.87	0.89	0.66	0.83	0.95	0.96	0.96	0.94	0.60	0.99
ANNA	rms	17.1	28.7	50.0	56.5	25.9	42.9	67.4	29.8	17.4	17.5	19.8	26.8	40.5	8.2
	E	5.1	12.2	37.4	45.9	17.1	20.6	56.4	21.7	5.4	5.1	6.2	16.0	47.8	1.2
	r	0.98	0.95	0.63	0.62	0.95	0.96	0.64	0.87	0.98	0.98	0.97	0.96	0.73	1.00
	s	0.97	0.94	0.79	0.75	0.91	0.90	0.72	0.88	0.97	0.97	0.97	0.92	0.69	0.99
CAMB	rms	17.5	22.0	69.9	74.2	22.2	41.5	57.3	23.3	16.9	19.5	27.7	30.6	35.0	22.7
	E	7.8	10.3	72.2	79.7	17.6	27.2	64.6	18.2	7.4	9.8	17.2	28.9	49.3	13.9
	r	0.97	0.93	0.32	0.35	0.92	0.87	0.56	0.88	0.97	0.92	0.84	0.85	0.67	0.90
	s	0.96	0.95	0.56	0.55	0.91	0.86	0.68	0.90	0.96	0.95	0.91	0.86	0.70	0.93
LEWI	rms	14.2	15.4	23.8	28.3	11.9	36.9	45.8	11.0	14.3	13.9	16.9	28.2	17.8	12.9
	E	7.1	8.7	25.5	36.6	7.2	30.1	51.6	5.6	7.4	6.9	9.9	43.2	18.4	6.7
	r	0.97	0.97	0.76	0.75	0.98	0.94	0.75	0.97	0.96	0.98	0.97	0.91	0.95	0.98
	s	0.96	0.96	0.86	0.83	0.96	0.85	0.75	0.97	0.96	0.97	0.95	0.80	0.90	0.97
HAMP	rms	13.6	10.8	41.7	38.1	12.1	36.9	42.3	18.2	12.5	13.7	18.3	30.1	23.2	18.8
	E	5.4	3.8	27.8	25.0	5.9	24.2	39.4	12.2	5.3	5.4	8.6	37.1	27.4	12.3
	r	0.97	0.98	0.87	0.85	0.97	0.91	0.72	0.89	0.97	0.97	0.97	0.88	0.91	0.93
	s	0.97	0.98	0.84	0.86	0.97	0.87	0.79	0.94	0.97	0.97	0.96	0.83	0.85	0.94
KIPT	rms	15.2	15.3	25.2	23.3	10.8	26.0	26.8	13.7	14.9	15.3	16.6	28.4	11.0	14.4
	E	13.9	15.1	27.0	23.8	8.1	30.9	38.6	12.6	14.5	14.0	16.0	84.4	9.6	15.4
	r	0.96	0.96	0.87	0.81	0.98	0.88	0.84	0.94	0.96	0.96	0.95	0.75	0.97	0.93
	s	0.93	0.93	0.86	0.87	0.96	0.85	0.82	0.94	0.93	0.93	0.92	0.63	0.95	0.92
CBBT	rms	12.3	11.0	34.9	38.1	10.0	29.0	30.3	13.1	11.0	12.4	13.3	31.2	16.4	19.8
	E	6.3	5.6	27.7	31.8	5.2	22.8	32.4	8.4	5.7	6.3	7.0	65.0	16.8	18.8
	r	0.96	0.97	0.87	0.80	0.97	0.89	0.76	0.93	0.97	0.96	0.97	0.84	0.91	0.91
	s	0.97	0.97	0.85	0.81	0.97	0.88	0.83	0.96	0.97	0.97	0.96	0.71	0.91	0.91

correlation coefficient in SLOW is less than 0.8 at most stations. This is not surprising since SLOW alters considerably the arrival time of peak surge as discussed in Section 4. On the other hand, FAST has relatively higher r values than those in SLOW. Besides the poor correlation, SLOW also generates much larger rms and E values than those in CTRL and FAST. This is a reflection of the long duration of high water level predicted by SLOW (see Figs. 8 and 9).

An analysis of runs in Group D demonstrates that coarse spatial resolution (36KM) in the MM5 lead to significant errors in the storm surge prediction, particularly in the narrow upper Bay region. In contrast, reducing the temporal resolution in the MM5 outputs from 1 to 6 h only leads to relatively modest degradation in the model's predictive skill.

Finally, a comparison between NTID and NWND in Group E shows that the predictive skill in NTID increases from the lower to upper Bay whereas the reverse is true in NWND. This difference is, of course, related to the fact that the incoming coastal storm surge affects the lower Bay whereas the local wind forcing dominates the response in the upper Bay. BIGC has the similar predictive skill as CTRL.

6. Concluding remarks

In this study, we have investigated how uncertainties in a hurricane model affect the storm surge prediction of a hydrodynamic model in a semi-enclosed bay. It is shown that small errors in the predicted hurricane parameters may lead to large errors in the storm surge prediction. Results indicate that the hurricane track and propagation speed are the two key factors in determining the storm surge response in a semi-enclosed bay. For a narrow semi-enclosed bay, such as Chesapeake Bay, the storm surge prediction is more sensitive to the spatial than temporal resolution of the horizontal wind field in a hurricane model.

The results presented herein have important implications for developing improved storm surge predictions, as more frequent and stronger hurricanes are expected to hit low-lying coastal regions in the future (Emanuel, 2005; Webster et al., 2005). Inner-coastal communities such as those living around Chesapeake Bay can be deceived by the idea that the extension of land seaward of enclosed bays and estuaries will protect inner-coastal residents and their property by blunting the power of storm surges approaching from the open sea. For some storm tracks, however, this same land extension can trap and even enhance surge height, such as the case of Hurricane Isabel on Chesapeake Bay. The sensitivity analyses presented in this paper highlight the challenges in predicting storm surges in the semi-enclosed bays and estuaries. Our results suggest that the ensemble forecasting technique, which has proven to be successful in improving weather forecasts, could be applied to the hydrodynamic models and may lead to improved predictions for storm surges.

Acknowledgements

We thank Dr. Shunli Zhang for his initial assistance in retrieving the MM5 real-time forecast data and NOAA for providing sea-level data at the tidal gauges. This work is supported by grants from NOAA (NA07NOS4730214), ONR and NSF (OCE-082543). This is UMCES contribution number 4434.

References

Boicourt, W.C., 2005. Physical response of Chesapeake Bay to hurricanes moving to the wrong side: refining the forecasts. In: Sellner, K.G. (Ed.), Hurricane Isabel in Perspective. CRC Publications No. 05-160. Chesapeake Research Consortium, Edgewater, MD, pp. 39–48.

Browne, D.R., Fisher, C.W., 1988. Tide and Tidal Currents in the Chesapeake Bay. NOAA Technical Report OS OMA 3. NOAA.

Chen, Q., Wang, L., Tawes, R., 2008. Hydrodynamic response of northeastern Gulf of Mexico to hurricanes. Estuaries and Coasts 31, 1098–1116.

Dudhia, J., 1989. Numerical study of convection observed during the winter monsoon experiments using a mesoscale two-dimensional model. Journal of Atmospheric Science 46, 3077–3107.

Egbert, G.D., Erofeeva, S.Y., 2002. Efficient inverse modeling of barotropic ocean tides. Journal of Atmospheric and Oceanic Technology 19, 183–204.

Emanuel, K.A., 2005. Increasing destructiveness of tropical cyclones over the past 30 years. Nature 436, 686–688.

Flather, R.A., Proctor, R., Wolf, J., 1991. Oceanographic forecast models. In: Famer, D.G., Rycroft, M.J. (Eds.), Computer Modeling in the Environmental Sciences. Oxford, U.K., pp. 15–30.

Garvine, R.W., 1985. A simple model of estuarine subtidal fluctuations forced by local and remote wind stress. Journal of Geophysical Research 90, 11945–11948.

Gerritsen, H., de Vries, H., Philippart, M., 1995. The Dutch continental shelf model. In: Lynch, D.R., Davies, A.M. (Eds.), Quantitative Skill Assessment for Coastal Ocean Models Coastal Estuarine Studies, vol. 47. American Geophysical Union, Washington, DC, pp. 425–467.

Grell, G.A., Dudhia, J., Stauffer, D.R., 1995. A Description of the Fifth-generation Penn State/NCAR Mesoscale Model (MM5). NCAR Technical Note NCAR/TN-398 1 STR. NCAR.

Holland, G.J., 1980. An analytical model of the wind and pressure profiles in hurricanes. Monthly Weather Review 108, 1212–1218.

Houston, S.H., Shaffer, W.A., Powell, M.D., Chen, J., 1999. Comparisons of HRD and SLOSH surface wind fields in hurricanes: implications for storm surge modeling. Weather and Forecasting 14, 671–686.

Hubbert, G.D., McInnes, K.L., 1999. A storm surge inundation model for coastal planning and impact studies. Journal of Coastal Research 15, 168–185.

Jelesnianski, C.P., Chen, J., Shaffer, W.A., 1992. SLOSH: Sea, Lake, and Overland Surges from Hurricanes. NOAA Technical Report NWS 48. NOAA, 71 pp.

Kain, J.S., Fritsch, J.M., 1993. Convective parameterization for mesoscale models: the Kain–Fritsch scheme, cumulus parameterization. Meteorological Monographs 46, 165–170.

Li, M., Zhong, L., Boicourt, W.C., 2005. Simulations of Chesapeake Bay estuary: sensitivity to turbulence mixing parameterizations and comparison with observations. Journal of Geophysical Research 110, C12004. doi:10.1029/2004JC002585.

Li, M., Zhong, L., Boicourt, W.C., Zhang, S., Zhang, D.-L., 2006. Hurricane-induced storm surges, currents and destratification in a semi-enclosed bay. Geophysical Research Letters 33, L02604. doi:10.1029/2005GL024992.

Li, M., Zhong, L., Boicourt, W.C., Zhang, S., Zhang, D.-L., 2007. Hurricane-induced destratification and restratification in a partially-mixed estuary. Journal of Marine Research 65, 169–192.

Oey, L.-Y., 2005. A wetting and drying scheme for POM. Ocean Modelling 9, 133–150.

Peng, M., Xie, L., Pietrafesa, L.J., 2004. A numerical study of storm surge and inundation in the Croatan-Albemarle-Pamlico Estuary System. Estuarine, Coastal and Shelf Science 59, 121–137.

Peng, M., Xie, L., Pietrafesa, L.J., 2006. Tropical cyclone induced asymmetry of sea level surge and fall and its presentation in a storm surge model with parametric wind fields. Ocean Modelling 14, 81–101.

Powell, M.D., Houston, S.H., Amat, L.R., Morisseau-Leroy, N., 1998. The HRD real-time hurricane wind analysis system. Journal of Wind Engineering and Industrial Aerodynamics 77, 53–64.

Rappaport, E.N., Franklin, J.L., Avila, L.A., et al., 2009. Advances and challenges at the National Hurricane Center. Weather and Forecasting 24, 395–419.

Scheffner, N.W., Fitzpatrick, P.J., 1997. Real-time predictions of surge propagation. In: Spaulding, M.L., Blumberg, A.F. (Eds.), Estuarine and Coastal Modeling 1997. ASCE, Reston, VA, pp. 374–388.

Shchepetkin, A.F., McWilliams, J.C., 2005. The Regional Oceanic Modeling System: a split-explicit, free-surface, topography-following-coordinate ocean model. Ocean Modelling 9, 347–404.

Shen, J., Wang, H., Sisson, M., Gong, W., 2006. Storm tide simulation in the Chesapeake Bay using an unstructured grid model. Estuarine, Coastal and Shelf Science 68, 1–16.

Spitz, Y.H., Klinck, J.M., 1998. Estimate of bottom and surface stress during a spring-neap tide cycle by dynamic assimilation of tide gauge observations in the Chesapeake Bay. Journal of Geophysical Research 103, 12761–12782.

Vested, H.J., Jensen, H.R., Petersen, H.M., 1992. An operational hydrographic warning system for the North Sea and the Danish Belts. Continental Shelf Research 12, 65–81.

Verboom, G.K., Ronde, J.G., Van Dijk, R.P., 1992. A fine grid tidal flow and storm surge model of the North Sea. Continental Shelf Research 12, 213–233.

Warner, J.C., Geyer, W.R., Lerczak, J.A., 2005. Numerical modeling of an estuary: a comprehensive skill assessment. Journal of Geophysical Research 110, C05001. doi:10.1029/2004JC002691.

Webster, P.J., Holland, G.J., Curry, J.A., Chang, H.R.-R., 2005. Changes in tropical cyclone number, duration, and intensity in a warming environment. Science 309, 1844–1846.

Weisberg, R.H., Zheng, L., 2006. Hurricane storm surge simulations for Tampa Bay. Estuaries and Coasts 29, 899–913.

Westerink, J.J., Luettich, R.A., Baptista, A.M., Scheffner, N.W., Farrar, P., 1992. Tide and storm surge predictions using a finite element model. Journal of Hydraulic Engineering 118, 1373–1390.

Xie, L., Pietrafesa, L.J., Peng, M., 2004. Incorporation of a mass-conserving inundation scheme into a three-dimensional storm surge model. Journal of Coastal Research 20, 1209–1223.

Zhang, D.-L., 1989. The effect of parameterized ice microphysics on the simulation of vortex circulation with a mesoscale hydrostatic model. Tellus 41A, 132–147.

Zhang, D., Anthes, R.A., 1982. A high-resolution model of the planetary boundary layer – sensitivity tests and comparisons with SESAME-79 data. Journal of Applied Meteorology 21, 1594–1609.

Zhang, D.-L., Chang, H.-R., Seaman, N.L., Warner, T.T., Fritsch, J.M., 1986. A two-way interactive nesting procedure with variable terrain resolution. Monthly Weather Review 114, 1330–1339.

Zhang, Y.-L., Baptista, A.M., Myers, E.P., 2004. A cross-scale model for 3D baroclinic circulation in estuary-plume-shelf systems: I. Formulation and skill assessment. Continental Shelf Research 24, 2187–2214.

Zhong, L., Li, M., 2006. Tidal energy fluxes and dissipation in the Chesapeake Bay. Continental Shelf Research 26, 752–770.

Zhong, L., Li, M., Foreman, M.G.G., 2008. Resonance and sea level variability in Chesapeake Bay. Continental Shelf Research 28, 2565–2573.